ADVANCES IN NUCLEAR SCIENCE AND APPLICATIONS

Volume 2, No. 1 (2026), P. 30-40

Sensitivity of the s-process termination point to neutron capture cross sections and irradiation parameters

R. Spassyuk[1], D. Anarbek[1,2], M. Khassanov[1,2],
Y. Aimuratov[1,2,3] *, N. Kenzhebayev[1,2], M. Abishev[1,2]

[1]Fesenkov Astrophysical Institute, Almaty, Kazakhstan

[2]Al-Farabi Kazakh National University, Almaty, Kazakhstan

[3]International Center for Relativistic Astrophysics Network, Pescara, Italy

e-mail: aimuratov@fai.kz

DOI: 10.63907/ansa.v2i1.68
Received: 25 January 2026

Abstract

The termination of the slow neutron capture process (s-process) in the Pb–Bi mass region plays a key role in shaping the abundances of the heaviest stable nuclei produced in stellar environments. In this work, we revisit the classical description of the s-process termination developed by Clayton and co-authors, incorporating modern experimental neutron capture cross sections and exploring the sensitivity of the results to variations in neutron irradiation parameters.

The reaction network describing the Pb–Bi–Po termination cycle is reformulated as a system of Bateman equations and solved numerically using the burn-up matrix formalism combined with the Padé approximation for the matrix exponential. We investigate the influence of updated (n, γ) cross sections for Pb and Bi isotopes, as well as variations in the shape and scale parameters of the neutron exposure distribution, on the isotopic abundances, the timescale required to reach equilibrium, and the behavior at maximum neutron exposure.

Our results confirm the robustness of the quasi-stationary equilibrium condition $\sigma_A N_A = \text{const}$ under modern nuclear data, while demonstrating that updated cross sections lead to a noticeable redistribution of isotopic abundances and modify the timescale for reaching the equilibrium plateau.

The contribution of the s-process termination to the total abundances of Pb and Bi isotopes is further examined using different neutron exposure

distributions. We find that the resulting s-process abundances are largely insensitive to the neutron capture cross section of ^{209}Bi over the investigated range, confirming that ^{208}Pb effectively acts as the termination point of the s-process. Among the considered exposure models, the exponential neutron exposure distribution provides the best overall description of the final s-process abundances. These results are in good agreement with observational abundance constraints and demonstrate that the main qualitative features of the classical Clayton scheme remain valid, while quantitative predictions are significantly refined by modern nuclear data and irradiation models.

1 Introduction

The study of the termination region of the slow neutron capture process (s-process) in the mass number range $A \simeq 204$–210 is of fundamental importance for understanding the origin of lead and bismuth isotopes under astrophysical conditions. Classical works by Clayton and co-authors [1–3] established an analytical framework for describing this region, demonstrating that once a stationary regime is reached in the Pb–Bi–Po reaction chain, the condition $\sigma_A N_A = \text{const}$ holds, and the dominant fraction of the neutron capture flow accumulates near the isotope ^{209}Bi.

The original Clayton's model is, however, limited by its reliance on neutron capture cross sections available at the time and by a simplified parametrization of neutron irradiation. In particular, the model employs fixed analytical forms of the neutron exposure distribution, which do not account for fluctuations in neutron flux intensity or for the diversity of astrophysical environments in which the s-process operates. Over the past decades, significantly more accurate experimental data for the (n, γ) cross sections of Pb and Bi isotopes have become available due to advances in nuclear measurements [4, 5], and are now compiled in modern evaluated nuclear data libraries such as MACS[1] and ENDF.[2]

In parallel, a wide range of neutron irradiation models has been developed in astrophysics [6–11]. These models reflect the diversity of physical conditions under which neutrons are produced and transported in stellar interiors and differ in the functional form of the neutron exposure distribution, as well as in the temporal structure and intensity of the neutron flux. Various parametrizations of neutron irradiation are employed in modeling the s-process in asymptotic giant branch (AGB) stars, both under radiative burning conditions, for example within the ^{13}C pockets, and during convective thermal pulses, where the ^{22}Ne(α, n) neutron source becomes active. In addition, distinct classes of irradiation models are applied to more extreme astrophysical scenarios associated with the intermediate and rapid neutron capture processes, denoted i-process [12–14] and r-process [15–19], correspondingly, which are characterized by substantially higher neutron densities and markedly different temporal organizations of neutron exposure.

In this work, we assess the robustness and sensitivity of the classical Clayton results with respect to above updates in nuclear data and controlled variations of the neutron exposure model parameters. Specifically, we investigate the impact of modern experimental (n, γ) neutron capture cross sections for Pb and Bi isotopes, as

[1] https://www.nndc.bnl.gov/astro/
[2] https://www-nds.iaea.org/exfor/endf.htm

well as variations in the shape (m) and scale (μ) parameters of the neutron exposure distribution [1–3]. To this end, the original reaction scheme is reformulated as a system of Bateman equations and expressed in terms of a burn-up matrix.

The paper is organized as follows. In Section 2, we provide a brief overview of the classical Clayton framework describing the termination of the s-process in the Pb–Bi region. The numerical methodology and the computational approach are described in Section 3. The results are presented in Section 4 and Section 5.

2 The termination of the s-process

In this section, the classical Clayton scheme describing the termination of the s-process in the Pb–Bi–Po region is introduced. The key physical assumptions underlying the model are discussed, including the neglect of unstable isotopes and the use of neutron exposure as the main parameter governing the process. Moreover, the adopted parametrization of neutron exposure and its role in shaping the isotopic dynamics and abundances near the termination point of the s-process are presented.

The pioneering work by Clayton and Rassbach [1] laid the foundation for the modern understanding of how the s-process terminates in the region of heavy lead and bismuth isotopes. Their scheme assumes that the last stable nuclide of the chain, ^{209}Bi, after capturing a neutron, enters a region of unstable masses, where the subsequent evolution is governed by the competition between β-decay and the following α-decay. A crucial assumption of the original scheme is the instantaneous return of the radioactive isotopes ^{209}Pb, ^{210}Bi, and ^{210}Po back into the chain of stable isotopes.

This approximation allows the isotopic evolution to be analytically reduced to a linear system of four coupled equations [1]:

$$\frac{d}{d\tau}\begin{pmatrix}\psi_{206}\\ \psi_{207}\\ \psi_{208}\\ \psi_{209}\end{pmatrix} = \begin{pmatrix}-\sigma_{206} & 0 & 0 & \sigma_{209}\\ \sigma_{206} & -\sigma_{207} & 0 & 0\\ 0 & \sigma_{207} & -\sigma_{208} & 0\\ 0 & 0 & \sigma_{208} & -\sigma_{209}\end{pmatrix}\begin{pmatrix}\psi_{206}\\ \psi_{207}\\ \psi_{208}\\ \psi_{209}\end{pmatrix} + \begin{pmatrix}1\\ 0\\ 0\\ 0\end{pmatrix}\sigma_{206}\psi_{205}, \tag{1}$$

where $\psi_A = \sigma_A N_A$ denotes the abundance of the isotope with mass number A.

To describe the temporal evolution of isotopic abundances governed by Eq. (1), the concept of neutron exposure τ is introduced [1, 7, 10, 20]. It represents the time-integrated neutron irradiation and is defined as

$$\tau = \int_0^t n_n(t)\, v_T(t)\, dt, \tag{2}$$

where $n_n(t)$ is the neutron density and $v_T(t)$ is the thermal neutron velocity.

According to Eq. (2), τ has the inverse dimension of a neutron capture cross section and effectively defines the probability for a nucleus to capture a neutron over the entire irradiation history. Under realistic astrophysical conditions, matter does not experience a single fixed neutron exposure, but rather a continuous distribution of exposure values [21, 22]. To account for this, a neutron exposure distribution function $\psi(\tau)$ is introduced [1], which is conventionally normalized as

$$\int_0^\infty \psi(\tau)\, d\tau = 1. \tag{3}$$

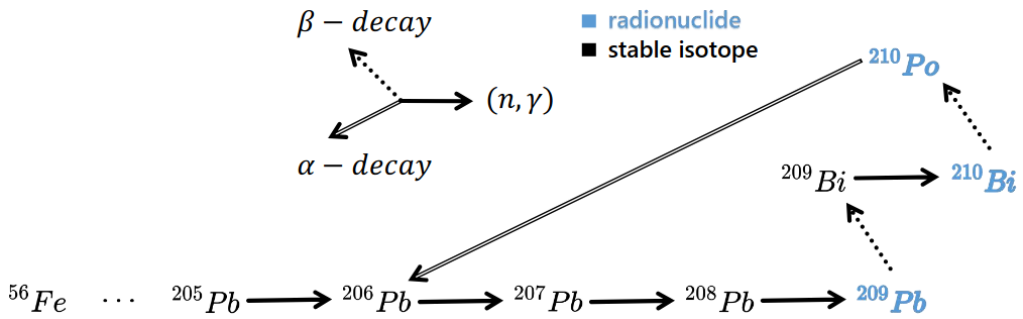

Figure 1: Schematic representation of the nuclear reaction chain occurring in the vicinity of the s-process termination point. Radioactive nuclides are highlighted in blue.

In work [1], the most universal and widely used parametrization in the form of a gamma distribution was adopted:

$$\psi_{205}(\tau) = \frac{\mu}{\Gamma(m)} (\mu\tau)^{m-1} e^{-\mu\tau}, \tag{4}$$

where $\Gamma(m)$ is the gamma function, μ is the scale parameter of the exposure, and m is the shape parameter (for $kT = 30$ keV, Clayton adopted $\mu_0 = 22.544$ mb and $m_0 = 35.397$ mb). The function ψ_{205} describes the production rate of the isotope ^{205}Pb as a function of neutron exposure τ. This parametrization is mathematically convenient and has therefore been widely employed in analytical studies of the s-process [1,3].

It allowed Clayton to demonstrate that, owing to the relatively low neutron capture cross sections of ^{208}Pb and ^{209}Bi, the main neutron capture flow is effectively stalled near ^{208}Pb, while the contribution of reaction paths proceeding through ^{210}Po remains negligible. The corresponding reaction scheme associated with Eq. (1) is shown in Figure 1.

3 Computational Methods

In this chapter, the framework used to describe the evolution of isotopic abundances in nuclear reaction chains is presented. On this basis, the subsequent analysis of isotopes transformation focuses on the temporal behavior in term of the Eq. (2). Within the framework of this study, the evolution of isotopic abundances is formulated based on the classical Bateman approach [23].

Let $N_i(t)$ denote the abundance of the i-th nuclide. The rate of change of $N_i(t)$ is then determined by radioactive decay, (n, γ) neutron capture processes, as well as by the production of nuclides arising from the transformations of other isotopes. The corresponding equation can be written as

$$\frac{dN_i(t)}{dt} = -\lambda_i N_i(t) - \sigma_i \phi N_i(t) + \sum_{j \neq i} \lambda_j P_{j \to i} N_j(t) + \sum_{j \neq i} \sigma_j \phi Q_{j \to i} N_j(t), \tag{5}$$

where λ_i is the decay constant of the i-th nuclide, σ_i is its neutron capture cross section, Φ is the neutron flux, and P_{ji} and Q_{ji} denote the probabilities of transition

from nuclide j to nuclide i via radioactive decay and neutron capture, respectively. Then the system can be written in a compact matrix form as

$$\frac{d}{dt}\mathbf{N}(t) = \mathbf{A}\mathbf{N}(t), \tag{6}$$

where the matrix $\mathbf{A}$ contains the elements associated with radioactive decays and neutron capture reactions and represents the so-called burn-up matrix, and $\mathbf{N}(t)$ is the vector of isotope concentrations, such as

$$\mathbf{N}(t) = (N_1, N_2, \ldots, N_I)^T . \tag{7}$$

The formal solution of this system Eq. (6) can be expressed in terms of the matrix exponential

$$\mathbf{N}(t) = \mathbf{N}_0 \exp(\mathbf{A}t) . \tag{8}$$

Since the direct computation of the matrix exponential $\exp(\mathbf{A}t)$ for large nuclear reaction networks is computationally demanding, specialized numerical methods are commonly employed [24, 25]. Among them, the so-called Padé approximation method [26] is one of the most efficient and widely used algorithms for evaluating the matrix exponential in burn-up calculations. The approach is based on a rational approximation of the matrix exponential, representing the function $\exp(\mathbf{A}t)$ as a ratio of two matrix polynomials. Padé approximations exhibit high accuracy for burn-up matrices, as the spectrum of such matrices $\mathbf{A}$ is predominantly located near the negative real axis, making the problem particularly well suited for this class of approximations.

In practical computations, Padé approximants of orders $(13, 13)$, $(16, 16)$, $(32, 32)$, or $(48, 48)$ are commonly employed, providing the required accuracy at reasonable computational cost even for strongly stiff systems of Bateman equations, see Eq. (5). The method is implemented in standard scientific Python libraries: the function `scipy.linalg.expm`[3] relies precisely on the Padé algorithm [27]. This makes it especially convenient for numerical modeling of nuclear burn-up and the evolution of nuclide chains, allowing the use of high-precision methods without the need for custom implementations.

4 Sensitivity Analysis

In this section, we examine the influence of the neutron exposure model parameters of shape (m) and scale (μ), as well as updated neutron capture cross sections, on the equilibrium abundance values of isotopes in the Pb–Bi–Po chain, the timescale required for the system to reach a stationary plateau, and the isotope abundances at the moment of maximum neutron irradiation $\tau_{\max}$ for the chain described by Eq. (1).

The baseline scenario adopts neutron exposure parameters $\mu = 22.544$ and $m = 35.397$, corresponding to the classical model of Ref. [1]. To assess the sensitivity of the results to the shape and scale of the neutron exposure, additional computational series were performed. These include variations of the exposure scale parameter μ over a wide range, from 1 to 100, while keeping the shape parameter fixed at

[3] https://docs.scipy.org/doc/scipy-1.2.3/reference/generated/scipy.linalg.expm.html

$m = 35.397$, as well as variations of the shape parameter m over a broad range while maintaining a fixed exposure scale parameter $\mu = 22.544$.

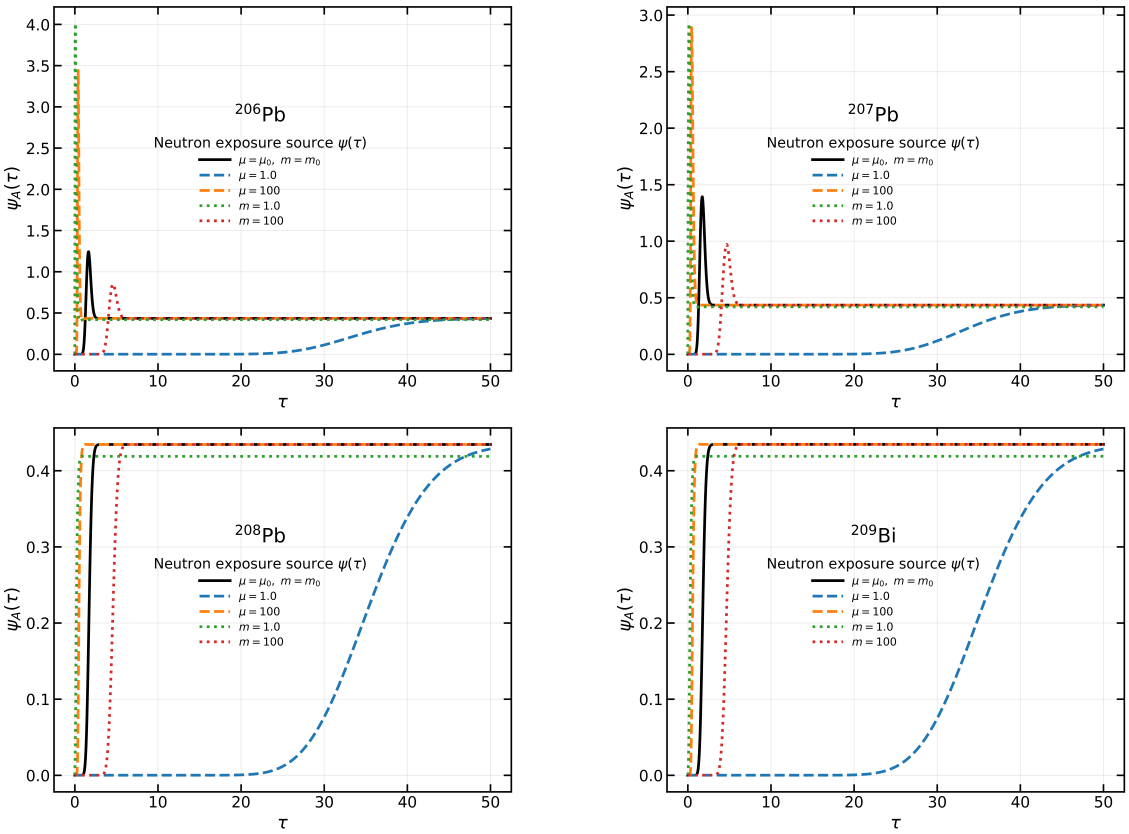

Figure 2: Evolution of the quantity ψ_A for the isotopes ^{206}Pb, ^{207}Pb, ^{208}Pb, and ^{209}Bi as a function of neutron exposure τ for different parameters of the neutron irradiation source model $\psi(\tau)$. The calculations are shown for the baseline parameter set adopted in Ref. [1] ($\mu = \mu_0$ and $m = m_0$), as well as for variations of the neutron exposure scale parameter μ ($\mu = 1$ and 100 at fixed $m = m_0$) and variations of the shape parameter m ($m = 1$ and 100 at fixed $\mu = \mu_0$).

As shown in Figure 2, variations in the parameters μ and m significantly affect the growth rate of the isotopic abundances, the position of the maximum, and the timescale required to reach the stationary plateau, while the equilibrium plateau of ψ_A is preserved for all isotopes.

In addition, all calculations were performed using both the set of neutron capture cross sections employed in Ref. [1] and (n, γ) cross-section data obtained from up-to-date nuclear databases, including the MACS[1] and ENDF[2]. The corresponding results are presented in Figure 3.

The results shown in Figure 3 (right panel) are in agreement with the classical solution of Clayton [1] (left panel), confirming the validity of the numerical approach based on the burn-up matrix and the Padé method. When updated neutron capture cross sections are employed, slight changes are observed in the relative abundances of the isotopes ^{206}Pb and ^{207}Pb, while much more pronounced differences appear for ^{208}Pb and ^{209}Bi. The timescale required to reach the equilibrium abundance plateau also changes: for the left panel of Figure 3 it is $\tau_{\rm pl} \simeq 2.75$, whereas for the right panel it is $\tau_{\rm pl} \simeq 3.75$. The time of plateau equilibrium is characterized by the condition

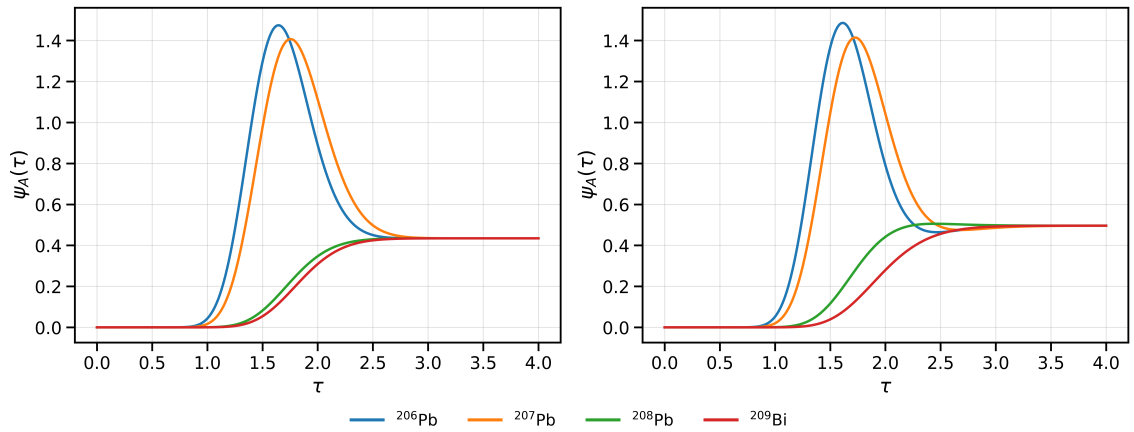

Figure 3: Temporal evolution of Pb–Bi isotopes under constant neutron irradiation. The abundances ψ_A are shown in units of mb×atom as a function of the neutron exposure parameter τ, expressed in units of 10^{27} n cm^{-2}, corresponding to the irradiation of a single target nucleus. The neutron capture cross sections correspond to a thermal energy of $kT = 30$ keV. The left panel shows the results obtained using the neutron capture cross sections adopted by Clayton [1]: $\sigma_{206} = 9.6$ mb, $\sigma_{207} = 8.7$ mb, $\sigma_{208} = 0.5$ mb, $\sigma_{209} = 12.1$ mb. The right panel presents the results based on modern evaluated cross-section data: $\sigma_{206} = 13.6$ mb, $\sigma_{207} = 8.266$ mb, $\sigma_{208} = 0.6569$ mb, $\sigma_{209} = 3.349$ mb. Updated neutron capture cross sections for the relevant isotopes were taken from the MACS[1] and ENDF[2].

$$\frac{dN_A(\tau)}{d\tau} = 0, \tag{9}$$

corresponding to a quasi-stationary equilibrium of the Pb–Bi termination cycle. Beyond these values, the abundance remains unchanged to the fourth decimal place. A more detailed comparison of the results is given in Table 1.

Table 1: Calculated equilibrium values ψ_A, [mb×atom] for the isotopes ^{206}Pb, ^{207}Pb, ^{208}Pb, and ^{209}Bi obtained using different sets of neutron capture cross sections. The established isotopic abundances at the moment of maximum neutron exposure $\tau_{\max}$ for the exposure model given by Eq. (4) are also listed.

Cross section	$\tau_{\max}$	τ_{pl}	^{206}Pb	^{207}Pb	^{208}Pb	^{209}Bi
Clayton [1]	1.6466	0.43	1.4674	1.3257	0.1592	0.1171
This work	1.6466	0.48	1.4688	1.3610	0.2152	0.0877

As can be seen from Table 1, the abundance of the isotope ^{209}Bi at the moment $\tau_{\max}$ decreases by approximately one order of magnitude when updated neutron capture cross sections are employed. The maximum abundances of ^{207}Pb and ^{208}Pb increase by 0.0353 mb×atom and 0.056 mb×atom, respectively, whereas the abundance of ^{206}Pb remains essentially unchanged.

The use of updated neutron capture cross sections therefore leads to a redistribution of isotopic abundances and modifies the timescale required to reach the equilibrium plateau. At the same time, both the equilibrium state and the peak and steady-state abundance values exhibit sensitivity to the updated nuclear data.

5 Contribution of the s-Process Termination to ^{206}Pb, ^{207}Pb, ^{208}Pb and ^{209}Bi Abundances

In this section, we analyze the contribution of the s-process to the formation of lead isotopic abundances due to the termination point of the s-process.

The number of iron seed nuclei exposed during the history of nucleosynthesis to an integrated neutron flux τ within the interval $d\tau$ is described by the distribution function $\rho(\tau)$. The total abundance produced by the s-process can then be written as

$$N_A = \frac{1}{\sigma_A} \int_0^\infty \rho(\tau)\, \psi_A(\tau)\, d\tau. \tag{10}$$

The function $\rho(\tau)$ represents the distribution of integrated neutron exposures experienced by seed nuclei during the s-process. We consider both an exponential exposure distribution

$$\rho(\tau) = 10^4 \, \exp\!\left(-\frac{\tau}{0.17}\right), \tag{11}$$

and a power-law distribution,

$$\rho(\tau) = 27.7\, \tau^{-3.18}. \tag{12}$$

Previously [1], the formation of the isotopes ^{206}Pb, ^{207}Pb, and ^{208}Pb within the framework of the s-process was investigated using neutron capture cross sections available at that time. It was shown that, at the termination point of the s-process, the total abundance of lead isotopes is largely insensitive to the neutron capture cross section of ^{208}Pb, which was poorly known at that time. Furthermore, within the adopted model of Ref. [1], the abundance of ^{208}Pb was found to be smaller than those of ^{206}Pb and ^{207}Pb.

In the present work, we re-evaluate these conclusions by exploring how the total abundances of ^{206}Pb, ^{207}Pb, and ^{208}Pb change when the neutron capture cross sections used in Ref. [1] are replaced by updated experimental data in MACS[1] and ENDF[2]. In contrast to the results of Ref. [1], modern astrophysical investigations of s-process nucleosynthesis and its termination indicate that the s-process provides the dominant contribution to the abundance of ^{208}Pb relative to ^{206}Pb and ^{207}Pb [15].

Analyses presented in Ref. [1] further indicate that for realistic neutron capture cross sections the s-process flow does not accumulate at ^{209}Bi due to the large value of $\sigma_{^{209}Bi}$. As a result, ^{208}Pb effectively acts as the termination point of the s-process, and ^{209}Bi was excluded from the analytical treatment in order to reduce computational complexity and obtain closed-form solutions. In the present study, we additionally examine whether the final abundances depend on the value of the neutron capture cross section of ^{209}Bi, noting that a value of ≈ 12.1 mb was used in Ref. [1], whereas modern evaluations yield values smaller by about a factor of four.

To evaluate Eq. (8), the set of isotopic solutions $\psi_A(\tau)$ obtained from Eq. (1) with using matrix exponential method [27] is substituted into Eq. (10) together with the chosen exposure distribution $\rho(\tau)$, yielding the total abundances produced by the s-process. The results of this analysis are presented in Figure 4.

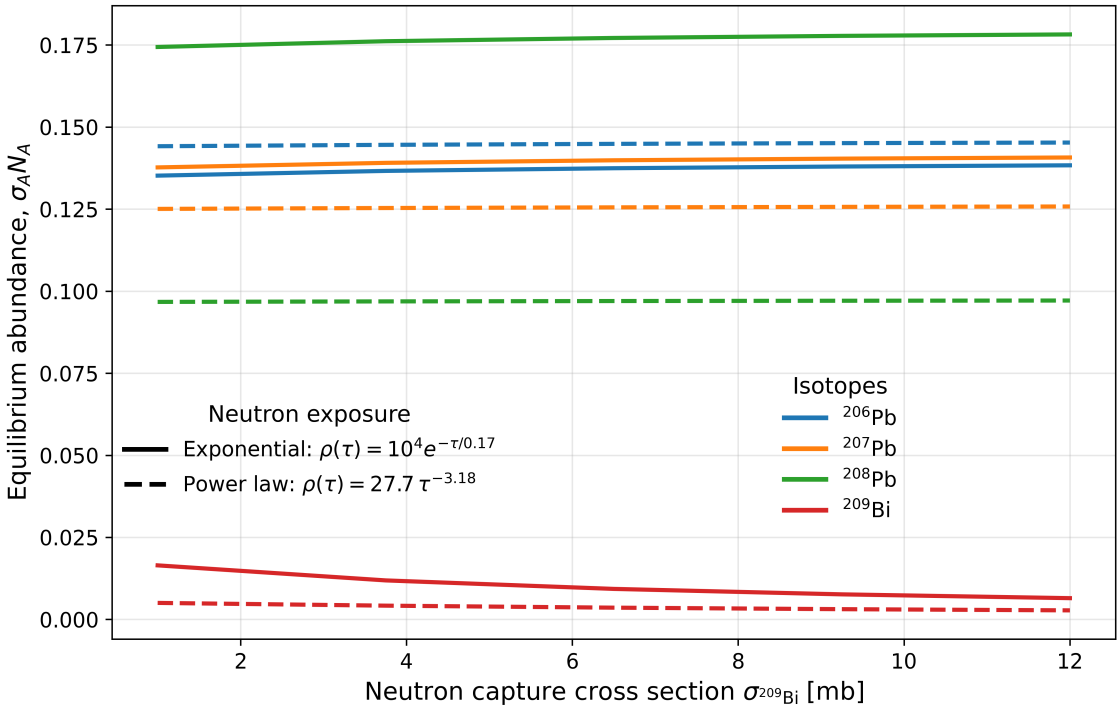

Figure 4: The s-process abundances of Pb and Bi isotopes obtained for two different characterizations of the neutron exposure distribution considered in Ref. [1]. In both cases, the resulting abundances are found to be nearly independent of the value of the neutron capture cross section of ^{209}Bi over the investigated range of cross-section values. The equilibrium concentrations was calculated for exponential and power-law $\rho(\tau)$ at $\tau \approx 4$ and 1.37, correspondingly.

According to Figure 4, the abundances $\sigma_A N_A$ are practically independent of the considered range of neutron capture cross section values of ^{209}Bi and remain at an approximately constant level. The corresponding equilibrium abundance values are summarized in Table 2.

Table 2: Equilibrium plateau values of $\sigma_A N_A$ in Figure 4 for Pb and Bi isotopes obtained for two characterizations of the neutron exposure distribution considered in Ref. [1].

Isotope	Exponential $\rho(\tau)$	Power-law $\rho(\tau)$
^{206}Pb	0.13664	0.14458
^{207}Pb	0.13909	0.12533
^{208}Pb	0.17615	0.096884
^{209}Bi	0.011887	0.0041930

In contrast to Ref. [1], we explicitly include the abundance of ^{209}Bi in our analysis. The exponential characterization of the neutron exposure distribution provides a good description of the resulting abundances. The final abundance of ^{208}Pb exceeds those of ^{206}Pb and ^{207}Pb, while the abundances of ^{206}Pb and ^{207}Pb remain comparable, in agreement with previous studies. The abundance of ^{209}Bi is found to be significantly smaller than those of the Pb isotopes. Overall, these results are consistent with the observed abundance patterns reported in Refs. [1, 15].

6 Conclusion

In this work, we have revisited the classical description of the termination of the s-process in the Pb–Bi region originally developed by Clayton et al. (1967) [1], incorporating updated neutron capture cross sections and exploring the sensitivity of the results to variations in the neutron exposure model. By reformulating the reaction network as a system of Bateman equations and solving it numerically using the burn-up matrix formalism and the Padé approximation, we obtained an accurate and flexible framework for analyzing both non-stationary and equilibrium isotopic abundances, see Sections 2 and 3.

Our calculations confirm that the condition of quasi-stationary equilibrium, $\sigma_A N_A = \text{const}$, remains valid when modern nuclear data are employed. However, the use of updated neutron capture cross sections leads to a noticeable redistribution of isotopic abundances and modifies the timescale required to reach the equilibrium plateau. This behavior is illustrated in Figure 3 for the neutron irradiation model given by Eq. (4). The corresponding results are presented in Section 4, see Fig. 3 and Table 1. An analysis of the irradiation model in Eq. (4) further shows that variations of its parameters do not affect the equilibrium abundance values themselves, but primarily influence the time required to reach the plateau and the position of the abundance maximum.

We further investigated the contribution of the s-process termination to the total abundances of Pb and Bi isotopes using different neutron exposure distributions. It was found that the resulting s-process abundances are largely insensitive to the neutron capture cross section of ^{209}Bi over the investigated range, which further confirms that ^{208}Pb effectively acts as the termination point of the s-process. The abundance of ^{209}Bi remains small for all considered exposure models, in agreement with observational abundance constraints [15]. When updated neutron capture cross sections are employed, the resulting isotopic ratios of ^{206}Pb, ^{207}Pb, and ^{208}Pb are found to be in good agreement with the observed solar system abundance pattern, with ^{208}Pb providing the dominant contribution. Among the considered neutron exposure distributions, the exponential form of $\rho(\tau)$ yields the best overall description of the final s-process abundances. These results are in good agreement with the observational abundance data reported in Ref. [15]. The corresponding results are presented in Section 5, see Fig. 4 and Table 2.

Overall, our study demonstrates that the main qualitative features of the classical Clayton's scheme are robust, while quantitative predictions are significantly refined by updated nuclear data and irradiation models. The presented work provides a consistent and versatile basis for future investigations of s-process termination under a wide range of astrophysical conditions.

Acknowledgments

This research was funded by the Science Committee of the Ministry of Science and Higher Education of the Republic of Kazakhstan under the Grant No. AP23488136 "The Energy Release of Cyclic Reactions of the Kilonova GW170817-GRB170817A-AT2017gfo").

References

[1] D. D. Clayton, M. E. Rassbach, Astrophys. J. **148**, 69 (1967).

[2] P. A. Seeger, W. A. Fowler, D. D. Clayton, Astrophys. J. Suppl. Ser. **11**, 121 (1965).

[3] D. D. Clayton, W. A. Fowler, T. E. Hull *et al.*, Ann. Phys. **12**, 331 (1961).

[4] C. Domingo-Pardo *et al.*, Phys. Rev. C **74**, 025807 (2006).

[5] L. Weissman *et al.*, Phys. Rev. C **96**, 015802 (2017).

[6] U. Ratzel *et al.*, Phys. Rev. C **70**, 065803 (2004).

[7] R. Gallino *et al.*, Astrophys. J. **497**, 388 (1998).

[8] C. Arlandini *et al.*, Astrophys. J. **525**, 886 (1999).

[9] C. Travaglio *et al.*, Astrophys. J. **601**, 864 (2004).

[10] S. Bisterzo *et al.*, Mon. Not. R. Astron. Soc. **404**, 1529 (2010).

[11] J. Barnes, B. D. Metzger, Astrophys. J. Lett. **939**, L29 (2022).

[12] M. Wiedeking *et al.*, Nat. Rev. Phys. **7**, 696 (2025).

[13] A. Choplin *et al.*, Eur. Phys. J. A **61**, 68 (2025).

[14] A. M. Riyas *et al.*, arXiv:2510.13339 (2025).

[15] H. Beer, F. Corvi, P. Mutti, Astrophys. J. **474**, 843 (1997).

[16] B. S. Meyer, J. S. Brown, Astrophys. J. Suppl. Ser. **112**, 199 (1997).

[17] R. Reifarth, C. Lederer, F. Käppeler, J. Phys. G **41**, 053101 (2014).

[18] J. Kuske, A. Arcones, M. Reichert, Astrophys. J. **990**, 37 (2025).

[19] N. Prantzos *et al.*, Mon. Not. R. Astron. Soc. **491**, 1832 (2020).

[20] F. Kaeppeler *et al.*, Astrophys. J. **257**, 821 (1982).

[21] W.-Y. Cui *et al.*, Chin. J. Astron. Astrophys. **7**, 224 (2007).

[22] M. Busso, R. Gallino, G. J. Wasserburg, Annu. Rev. Astron. Astrophys. **37**, 239 (1999).

[23] C.-A. Cruz-López, G. Espinosa-Paredes, Nucl. Eng. Technol. **54**, 275 (2022).

[24] P. Maria, Nucl. Sci. Eng. **182**, 297 (2016).

[25] C. Moler, C. van Loan, SIAM Rev. **45**, 3 (2003).

[26] M. Arioli, B. Codenotti, C. Fassino, Linear Algebra Appl. **240**, 111 (1996).

[27] A. H. Al-Mohy, N. J. Higham, SIAM J. Matrix Anal. Appl. **31**, 970 (2010).